

# Report worksheet 5

Joaquín Rapela

January 29, 2025

## Exercise 1: z-scored binned spikes

Figure 1 shows the zscores of the binned spikes of all neurons (bin size=1 sec, unsorted neurons). I chose `zmin` and `zmax` as the 1% and 99% percentiles of the zscores distribution, because, as shown below, negative z-values are informative.

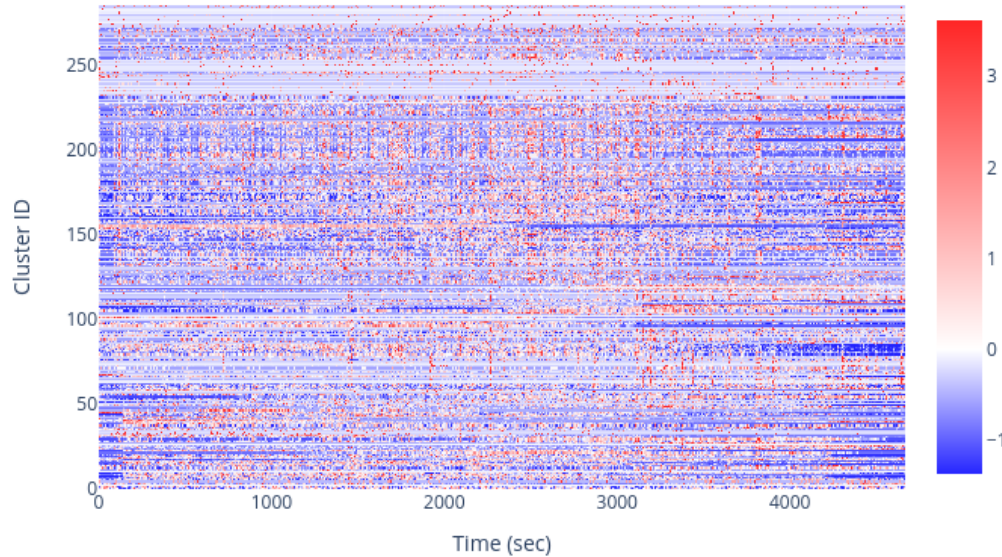


Figure 1: z-scores of binned spikes times of all neurons (bin size=1 sec, unsorted neurons). Generated with [this](#) script using its default parameters. Click on the image to see its interactive version.

If I don't limit the `zmax` of the heatmap colours become imbalanced due to a neuron with high firing at one time (Figure 2).

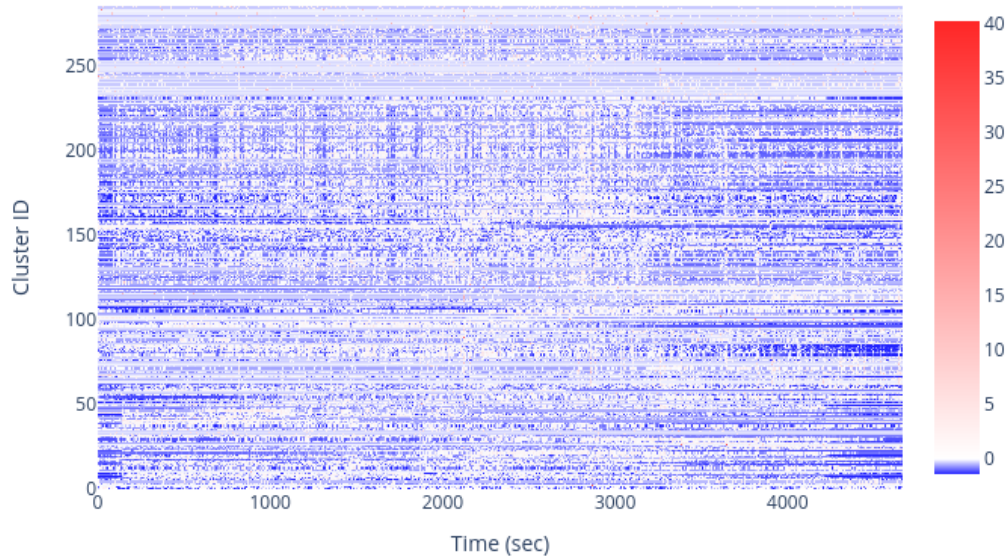


Figure 2: z-scores of binned spikes times of all neurons, plotted without `zmax` (bin size=1 sec, unsorted neurons). Generated with [this](#) script using its default parameters. Click on the image to see its interactive version.

If I don't z-score the binned spikes colours become imbalanced due to neurons that have large mean firing rate (Figure 3).

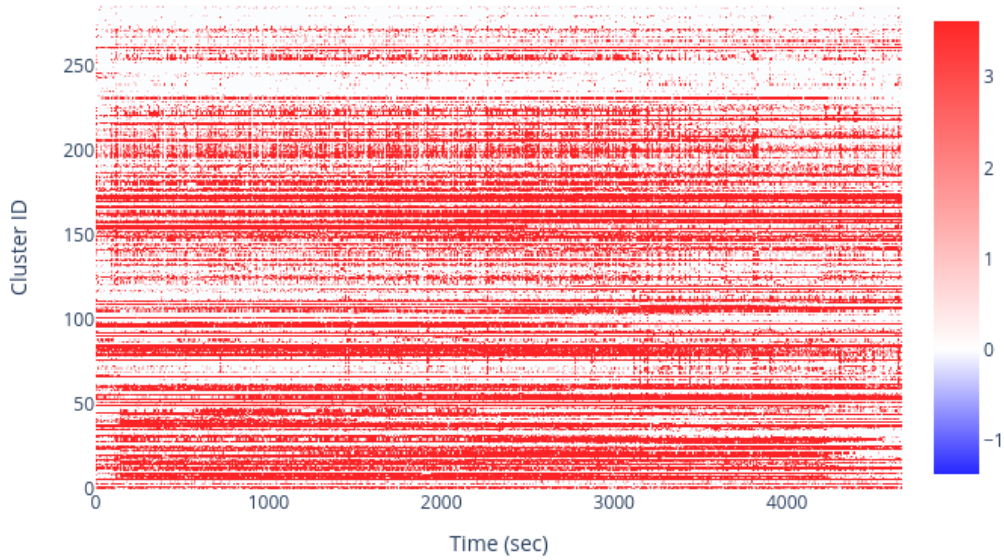


Figure 3: Non-zscored binned spikes times of all neurons (bin size=1 sec, unsorted neurons). Generated with [this](#) script using its default parameters. Click on the image to see its interactive version.

## Exercise 2: application of the SVD to z-scored binned spikes

Figure 4 plots the same z-scored binned spikes of Figure 1, but with neurons ordered according to their weight along the first right singular vector.

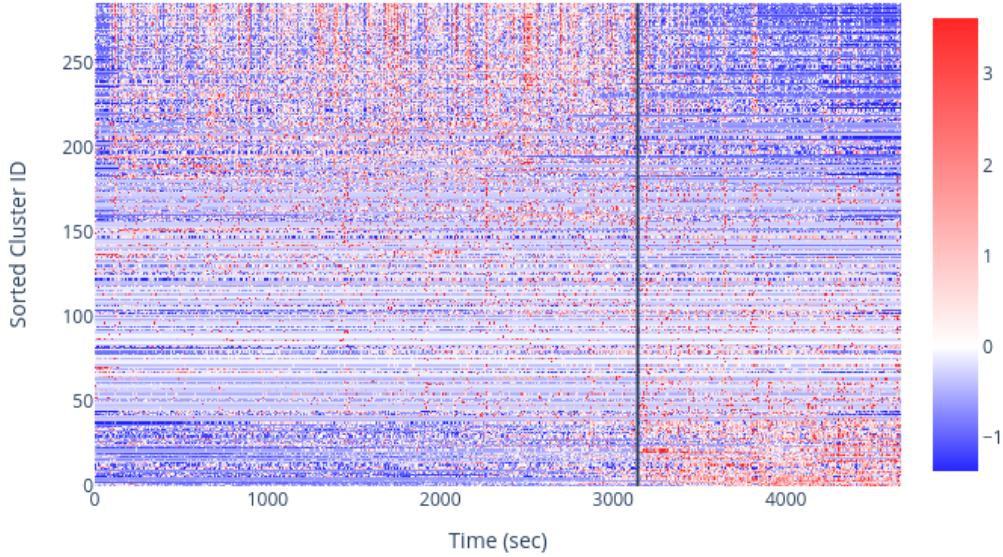


Figure 4: Same as Figure 1, but neurons have been sorted according to their weight along the first left singular vector. The black vertical line indicates the last response time of the subject. Generated with [this](#) script using its default parameters. Click on the image to see its interactive version.

The first left right singular vector (scaled by the corresponding entry in the first right singular vector) gives the temporal profile of the best rank-one approximation of the binned spikes of any neuron. Figure 5 plots in blue a part of the the first left singular vector between 400 and 650 seconds. The block vertical lines indicate subject response times. Interestingly, we see that this approximation of the binned spikes times tends to peak immediately after the subject response times. This suggest a synchronisation between neurons' spikes and subject's responses.

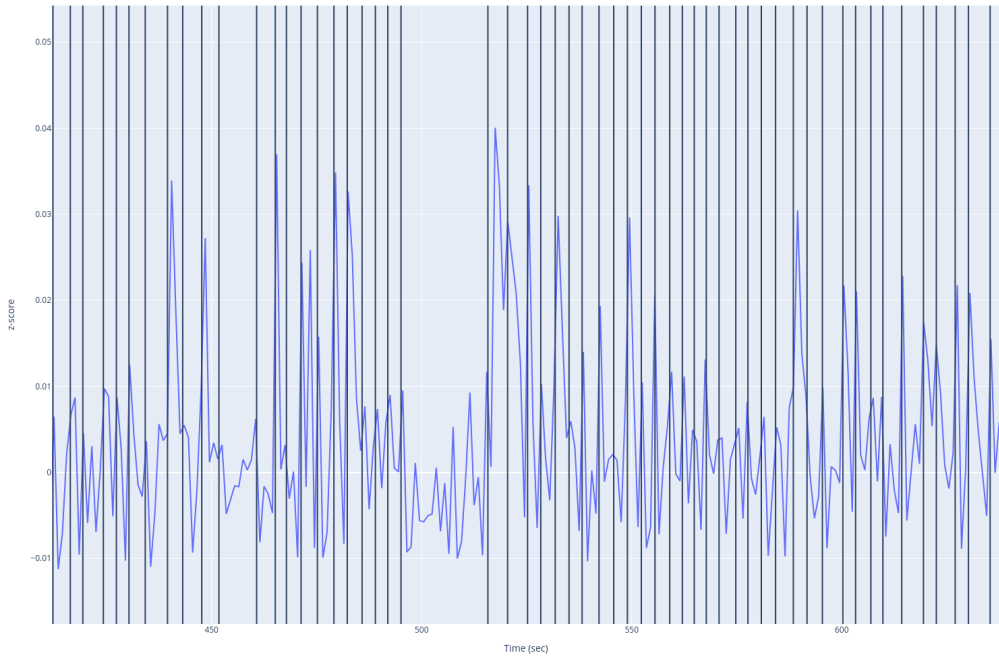


Figure 5: Part of the first left singular vector (blue trace) and subject response times (black vertical lines). This figure suggests a synchronisation between neurons' spikes and subjects responses (see text). Generated with [this](#) script using its default parameters. Click on the image to see its interactive version.

The  $n$ th entry of the first right singular vector gives us the weight of the first left singular vector to approximate the z-scores of the binned spikes of neuron  $n$ . Figure 6 plots the histogram of entries of the first right singular vector. We see weights as positive as 0.13, corresponding to neurons with z-scored binned spikes correlated to the first left singular vector. We also see weights as negative as -0.12, corresponding to neurons with z-scored binned spikes anti correlated to the first left singular vector.

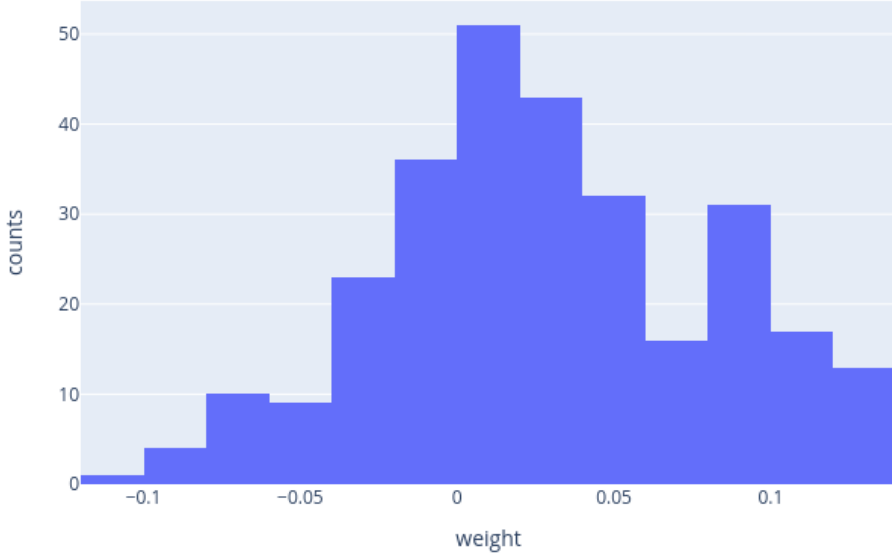


Figure 6: Histogram of entries in the first right left singular vector. Generated with [this](#) script using its default parameters. Click on the image to see its interactive version.

The weight of the first left singular vector on the z-scored binned spikes of the neurons near the top of Figure 4 is large and positive. We see vertical red stripes on the z-scores of these neurons, indicating their strong synchronisation with the response times of the subject. Before the time of the last response of the subject (black vertical line) z-scores tend to be positive (i.e., binned spikes larger than their mean), but after the last response of the subject z-scores tend to be negative. Moving the computer cursor over the top of the figure shows that most of these neurons belong to the primary motor cortex<sup>1</sup> and striatum<sup>2</sup>.

The opposite happens to neurons near the bottom of Figure 4. For these neurons the weight of the first left singular vector on their z-scored binned spikes is large and negative. We don't see vertical stripes on their z-scores. Before the time of the last response of the subject (black vertical line) z-scores tend to be negative (i.e., binned spikes lower than their mean), but after the last response of the subject z-scores tend to be positive. Moving the computer cursor over the top of the figure shows that most neurons belong to the pallidum<sup>3</sup>.

---

<sup>1</sup>areas: MOp5 (layer 5), MOp6a (layer 6a), MOp6b (layer 6b)

<sup>2</sup>areas: CP (caudoputamen), STR (striatum)

<sup>3</sup>area BST (bed nuclei of the stria terminalis)

## Appendix A Notes on the SVD

**Definition 1** (The SVD). *Given  $M \in \mathbb{C}^{m \times n}$ , a singular value decomposition (SVD) of  $M$  is a factorisation:*

$$M = USV^*$$

where

$$\begin{aligned} U &\in \mathbb{C}^{m \times m} \text{ is unitary,} \\ V &\in \mathbb{C}^{n \times n} \text{ is unitary,} \\ S &\in \mathbb{C}^{m \times n} \text{ is diagonal.} \end{aligned}$$

In addition, it is assumed that the diagonal entries  $s_k$  of  $S$  are nonnegative and in nonincreasing order; that is,  $s_1 \geq s_2 \geq \dots \geq s_p \geq 0$ , where  $p = \min(m, n)$ .

**Definition 2** (Rank of a matrix). *The column rank of a matrix is the dimension of the space spanned by its columns. Similarly, the row rank of a matrix is the dimension of the space spanned by its rows. The column rank of a matrix is always equal to its row rank. This is a corollary of the SVD. So we refer to this number simply as the rank of a matrix.*

The rank of a matrix can be interpreted as a measure of the complexity of the matrix. Matrices with lower rank are simpler than those with larger rank.

The SVD decomposes a matrix as a sum of rank-one (i.e., very simple) matrices.

$$M = \sum_{k=1}^r s_k \mathbf{u}_k \mathbf{v}_k^*$$

There are multiple other decompositions as sums of rank-one matrices. If  $M \in \mathbb{C}^{m \times n}$ , then it can be decomposed as a sum of  $m$  rank-one matrices given by its rows (i.e.,  $M = \sum_{i=1}^m \mathbf{e}_i \mathbf{m}_{i,\cdot}^*$ , where  $\mathbf{e}_i$  is the  $m$ -dimensional canonical unit vector, and  $\mathbf{m}_{i,\cdot}$  is the  $i$ th row of  $M$ ), or as a sum of  $n$  rank-one matrices given by its columns (i.e.,  $M = \sum_{j=1}^n \mathbf{m}_{\cdot,j} \mathbf{e}_j^*$ , where  $\mathbf{e}_j$  is the  $n$ -dimensional canonical unit vector, and  $\mathbf{m}_{\cdot,j}$  is the  $j$ th column of  $M$ ), or a sum of  $mn$  rank-one matrices each containing only one non-zero element (i.e.,  $M = \sum_{i=1}^m \sum_{j=1}^n m_{ij} E_{ij}$ , where  $E_{ij}$  is the matrix with all entries equal to zero, except the  $ij$  entry that is one, and  $m_{ij}$  is the entry of  $M$  at position  $ij$ ).

A unique characteristic of the SVD compared to these other decompositions is that, if the rank of a matrix is  $r$ , then its SVD yields optimal approximations of lower rank  $\nu$ , for  $\nu = 1, \dots, r$ , as shown by Theorem 1.

**Definition 3** (Frobenius norm). *The Frobenius norm of matrix  $M \in \mathbb{C}^{m \times n}$  is*

$$\|M\|_F = \left( \sum_{i=1}^m \sum_{j=1}^n m_{ij}^2 \right)^{1/2}$$

Note that

$$\|M\|_F = \sqrt{\text{tr}(M^* M)} = \sqrt{\text{tr}(MM^*)} \quad (1)$$

**Lemma 1** (Orthogonal matrices preserve the Frobenius norm). *Let  $M \in \mathbb{C}^{m \times n}$  and let  $P \in \mathbb{C}^{m \times m}$  and  $Q \in \mathbb{C}^{n \times n}$  be orthogonal matrices. Then*

$$\|PMQ\|_F = \|M\|_F$$

*Proof.*

$$\|PMQ\|_F = \sqrt{\text{tr}((PMQ)(PMQ)^*)} = \sqrt{\text{tr}(PMQ Q^* M^* P^*)} = \sqrt{\text{tr}(PMM^* P^*)} \quad (2)$$

$$= \sqrt{\text{tr}(P^* P M M^*)} = \sqrt{\text{tr}(MM^*)} = \|M\|_F \quad (3)$$

Notes:

1. The first equality in Eq. 2 follows Eq. 1.
2. The second equality in Eq. 2 uses the fact that  $(AB)^* = B^* A^*$ .
3. The third equality in Eq. 2 holds because  $Q$  is orthogonal (i.e.,  $QQ^* = I$ ).
4. The first equality in Eq. 3 uses the cyclic property of the trace (i.e.,  $\text{tr}(ABC) = \text{tr}(CAB)$ ).
5. The first equality in Eq. 3 holds by the orthogonality of  $P$ .
6. The last equality in Eq. 3 again applies Eq. 1.

□

A direct consequence of Lemma 1 is that the Frobenius norm of any matrix  $M = USV^*$  is

$$\|M\|_F = \|USV^*\|_F = \|S\|_F = \sqrt{\sum_{k=1}^r s_k^2}$$

Another consequence of Lemma 1 is the error in approximating a matrix  $M$  of rank  $r$  with its truncated SVD of rank  $\nu$  (i.e.,  $M_\nu = \sum_{k=1}^\nu s_k \mathbf{u}_k \mathbf{v}_k^*$ ) is

$$\|M - M_\nu\|_F = \left\| \sum_{k=1}^r s_k \mathbf{u}_k \mathbf{v}_k^* - \sum_{k=1}^\nu s_k \mathbf{u}_k \mathbf{v}_k^* \right\|_F = \left\| \sum_{k=\nu+1}^r s_k \mathbf{u}_k \mathbf{v}_k^* \right\|_F = \sqrt{\sum_{k=\nu+1}^r s_k^2} \quad (4)$$

**Theorem 1** (Eckart-Young-Mirsky). Let  $M \in \mathbb{C}^{m \times n}$  be of rank  $r$  with singular value decomposition  $M = \sum_{k=1}^r s_k \mathbf{u}_k \mathbf{v}_k^*$ . For any  $\nu$  with  $0 \leq \nu \leq r$ , define

$$M_\nu = \sum_{k=1}^\nu s_k \mathbf{u}_k \mathbf{v}_k^*$$

Then

$$\|M - M_\nu\|_F = \inf_{\substack{\tilde{M} \in \mathbb{C}^{m \times n} \\ \text{rank}(\tilde{M}) \leq \nu}} \|M - \tilde{M}\|_F = \sqrt{\sum_{k=\nu+1}^r s_k^2} \quad (5)$$

*Proof.* We use the Weyl's inequality that relates the singular values of a sum of two matrices to the singular values of each of these matrices. Precisely, if  $X, Y \in \mathbb{C}^{m \times n}$  and  $s_i(X)$  is the  $i$ th singular value of  $X$ , then

$$s_{i+j-1}(X + Y) \leq s_i(X) + s_j(Y) \quad (6)$$

Let  $\tilde{M}$  be a matrix of rank at most  $\nu$ . Applying Eq. 6 to  $X = M - \tilde{M}$ ,  $Y = \tilde{M}$  and  $j - 1 = \nu$  we obtain

$$s_{i+\nu}(M) \leq s_i(M - \tilde{M}) + s_{\nu+1}(\tilde{M}) = s_i(M - \tilde{M}) \quad (7)$$

The last equality in Eq. 7 holds because  $\tilde{M}$  has rank less or equal to  $\nu$ , and therefore its  $\nu + 1$  singular value is zero.

$$\begin{aligned} \|M - M_\nu\|_F^2 &= \sum_{j=\nu+1}^r s_j^2(M) = \sum_{i=1}^{r-\nu} s_{i+\nu}^2(M) \leq \sum_{i=1}^{r-\nu} s_i^2(M - \tilde{M}) \leq \sum_{i=1}^{\min(m,n)} s_i^2(M - \tilde{M}) \quad (8) \\ &= \|M - \tilde{M}\|_F^2 \end{aligned} \quad (9)$$

Notes:

1. The first equality in Eq. 8 holds by Eq. 4.
2. The second equality in Eq. 8 used the change of variables  $i = j - \nu$ .

3. The first inequality in Eq. 8 used Eq. 7
4. The last inequality in Eq. 8 is true because  $r - \nu \leq \min(m, n)$  and adding squared singular values to the sum in the left hand side only increases this sum.
5. The equality in Eq. 9 again holds by Eq. 5 and by the fact that singular values of index larger than the rank of a matrix are zero.

The last equality in Eq. 5 follows from Eq. 4.

□

## Appendix B Verification of the Eckart-Young-Mirsky theorem

I found it almost unbelievable that Theorem 1 allows us to compute the error that will be achieved by a low-rank approximation by just using the singular values of the matrix to be approximated, and without the need to calculating this approximation.

To verify Theorem 1, for different ranks  $\nu$ , I computed truncated SVD approximations to the matrix shown in Figure 4. For each of these approximations, I calculated the empirical error (i.e., the Frobenius norm of the difference between the matrix and the approximation) and the analytical error (i.e., the sum of singular values in Eq. 5). As shown in Figures 7-26 the empirical and analytical errors are almost identical.

analytical error: 1084.569150102873, empirical error: 1084.5691501028728

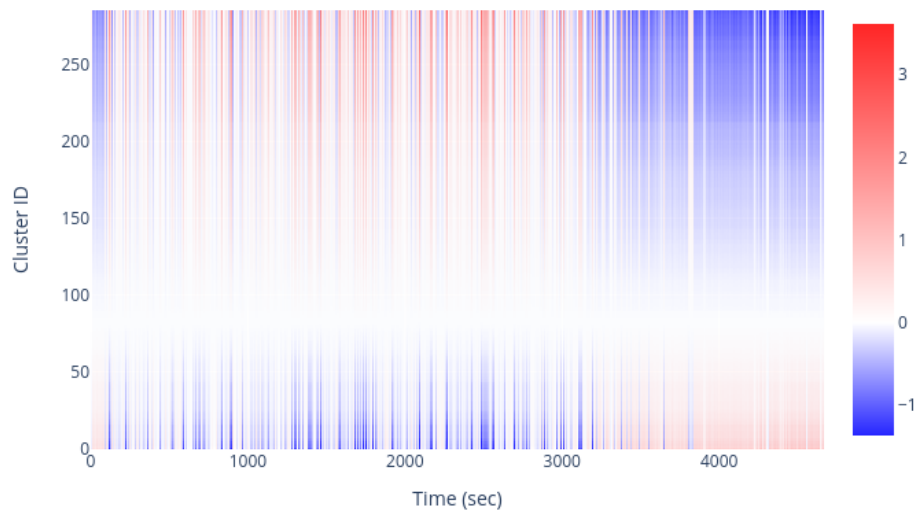


Figure 7: Low-rank approximation of the image in Figure 4 using a truncated SVD or rank 1. The title reports the empirical and analytical errors of the reconstruction. The empirical error is the Frobenius norm of the difference between the low-rank approximation and the image in Figure 4. The analytical error is computed from the singular values of the image in Figure 4 using Eq. 5. Generated with [this](#) script with [these](#) parameters. Click on the image to access its interactive version.

analytical error: 1023.4309570847728, empirical error: 1023.4309570847726

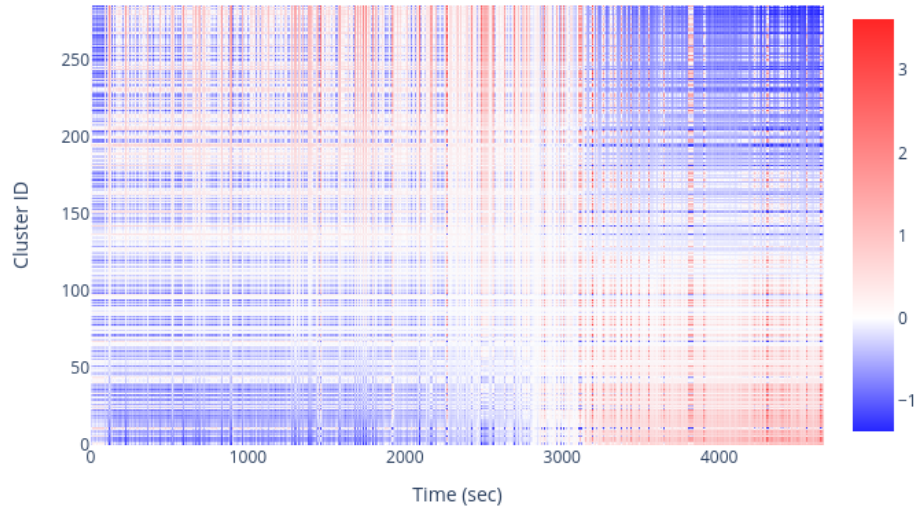


Figure 8: Low-rank approximation of the image in Figure 4 using a truncated SVD or rank 2. Same format as that in Figure 7. Click on the image to access its interactive version.

analytical error: 1001.2695900636994, empirical error: 1001.2695900636994

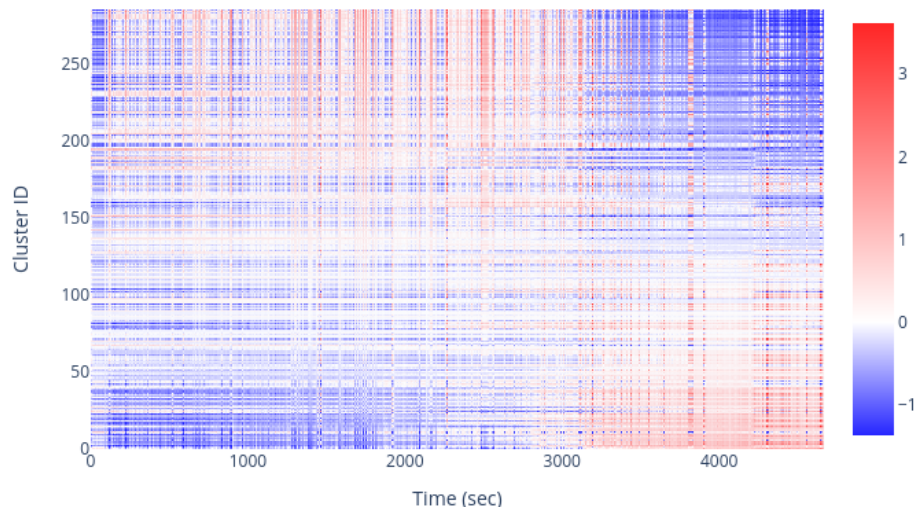


Figure 9: Low-rank approximation of the image in Figure 4 using a truncated SVD or rank 3. Same format as that in Figure 7. Click on the image to access its interactive version.

analytical error: 986.6766508924735, empirical error: 986.6766508924735

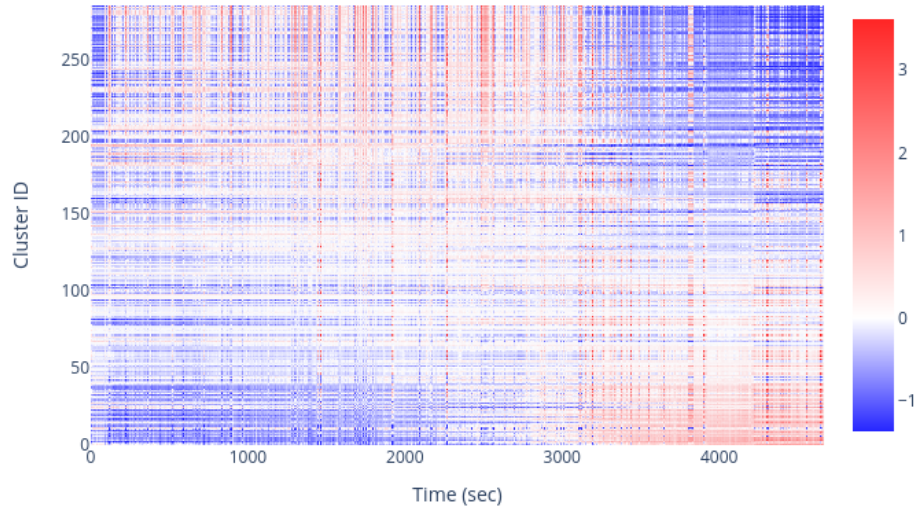


Figure 10: Low-rank approximation of the image in Figure 4 using a truncated SVD or rank 4. Same format as that in Figure 7. Click on the image to access its interactive version.

analytical error: 973.9474170608712, empirical error: 973.9474170608711

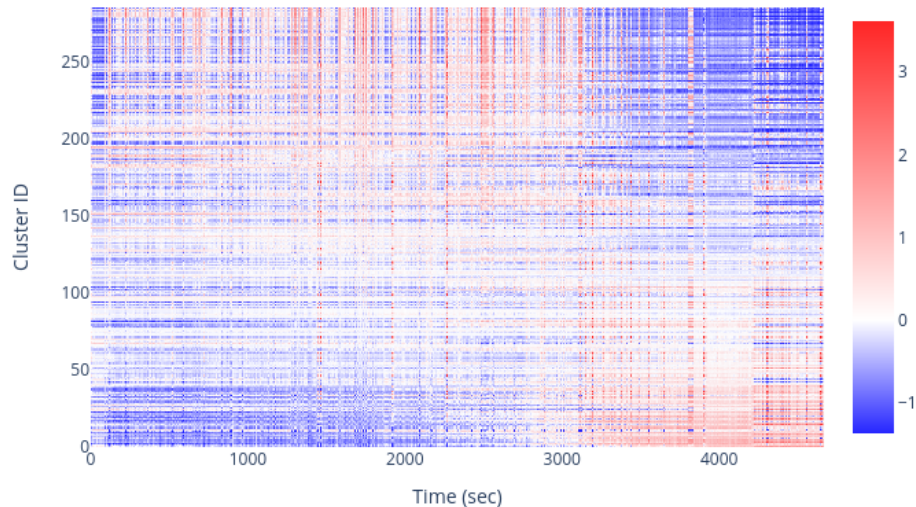


Figure 11: Low-rank approximation of the image in Figure 4 using a truncated SVD or rank 5. Same format as that in Figure 7. Click on the image to access its interactive version.

analytical error: 963.0187690622251, empirical error: 963.018769062225

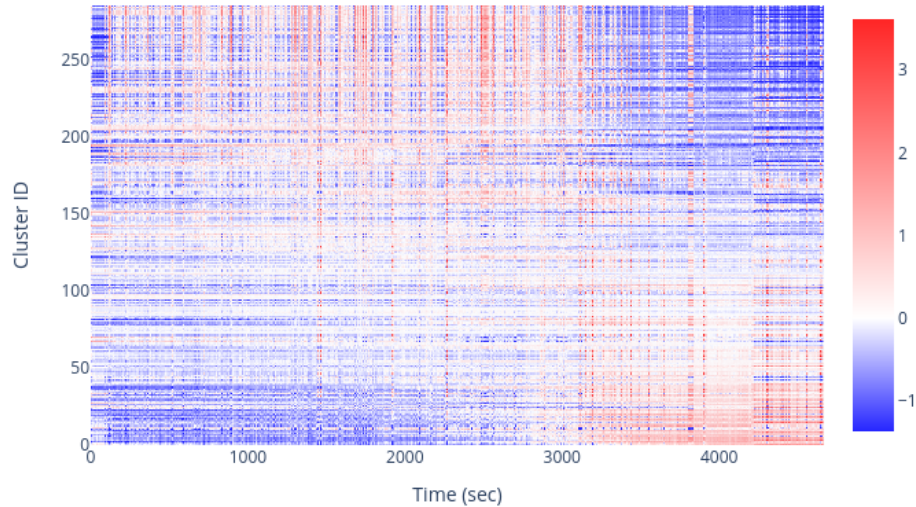


Figure 12: Low-rank approximation of the image in Figure 4 using a truncated SVD or rank 6. Same format as that in Figure 7. Click on the image to access its interactive version.

analytical error: 953.4685451393349, empirical error: 953.4685451393349

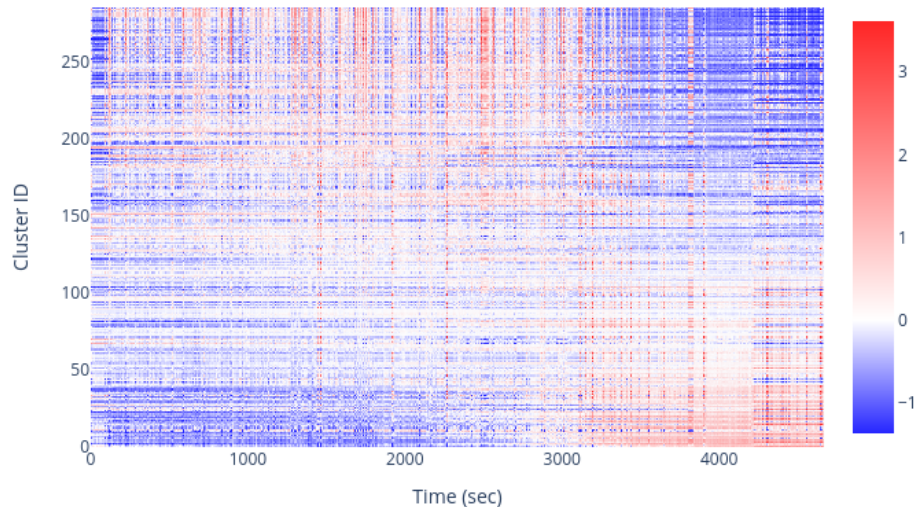


Figure 13: Low-rank approximation of the image in Figure 4 using a truncated SVD or rank 7. Same format as that in Figure 7. Click on the image to access its interactive version.

analytical error: 944.4365042298958, empirical error: 944.4365042298956

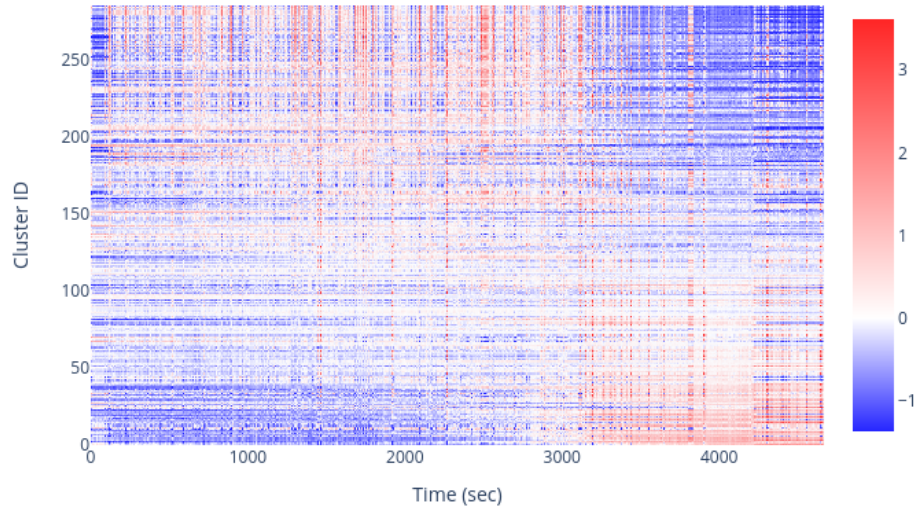


Figure 14: Low-rank approximation of the image in Figure 4 using a truncated SVD or rank 8. Same format as that in Figure 7. Click on the image to access its interactive version.

analytical error: 937.2332852848948, empirical error: 937.2332852848948

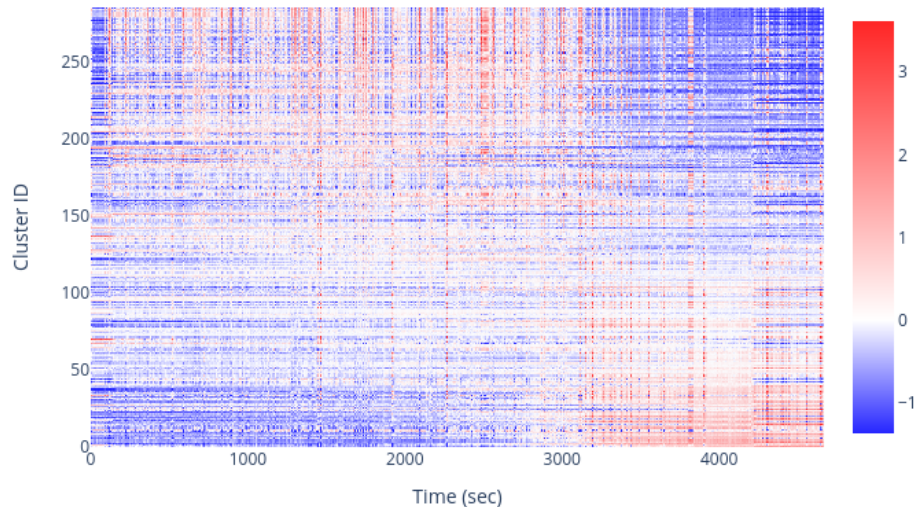


Figure 15: Low-rank approximation of the image in Figure 4 using a truncated SVD or rank 9. Same format as that in Figure 7. Click on the image to access its interactive version.

analytical error: 930.5395568142643, empirical error: 930.5395568142641

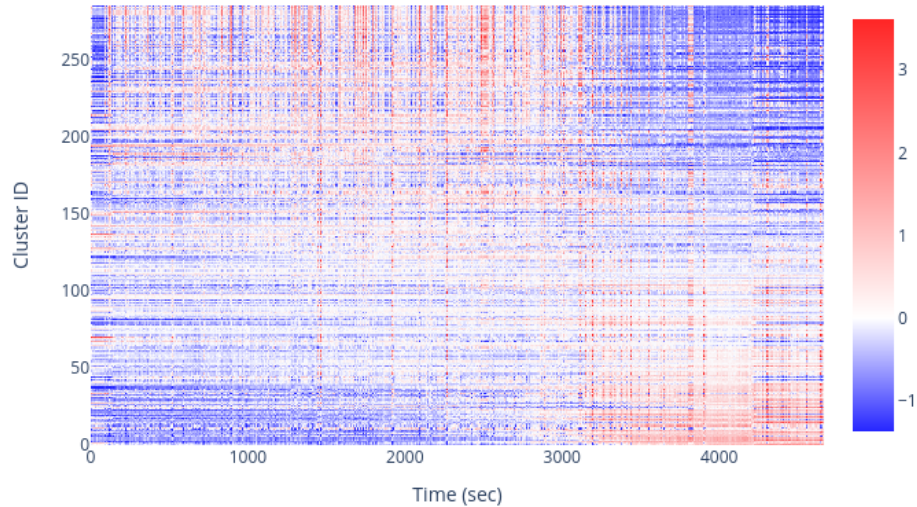


Figure 16: Low-rank approximation of the image in Figure 4 using a truncated SVD or rank 10. Same format as that in Figure 7. Click on the image to access its interactive version.

analytical error: 924.2095805256234, empirical error: 924.2095805256236

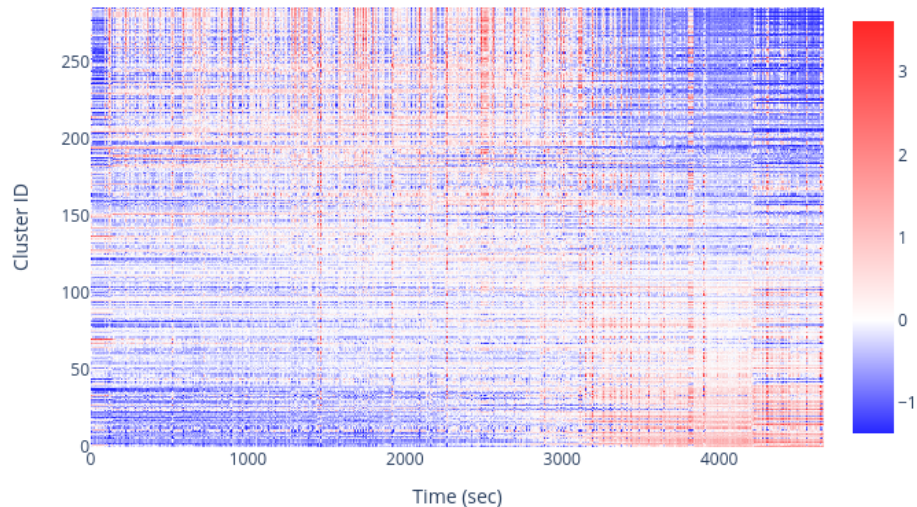


Figure 17: Low-rank approximation of the image in Figure 4 using a truncated SVD or rank 11. Same format as that in Figure 7. Click on the image to access its interactive version.

analytical error: 918.4024580402679, empirical error: 918.4024580402678

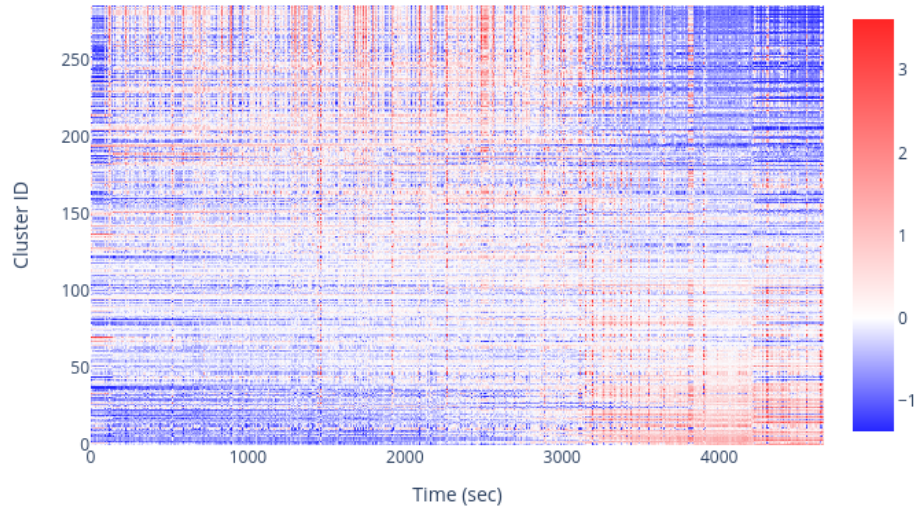


Figure 18: Low-rank approximation of the image in Figure 4 using a truncated SVD or rank 12. Same format as that in Figure 7. Click on the image to access its interactive version.

analytical error: 912.7932902557615, empirical error: 912.7932902557615

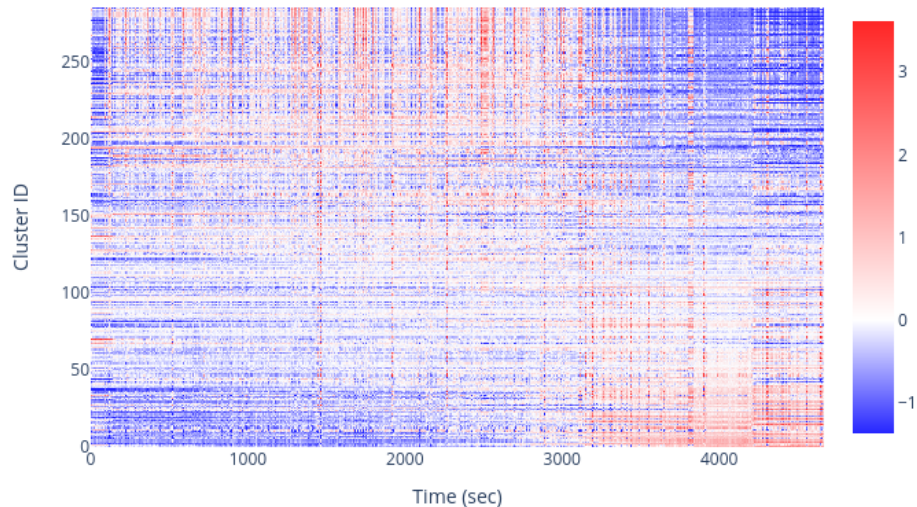


Figure 19: Low-rank approximation of the image in Figure 4 using a truncated SVD or rank 13. Same format as that in Figure 7. Click on the image to access its interactive version.

analytical error: 907.3483122478424, empirical error: 907.3483122478424

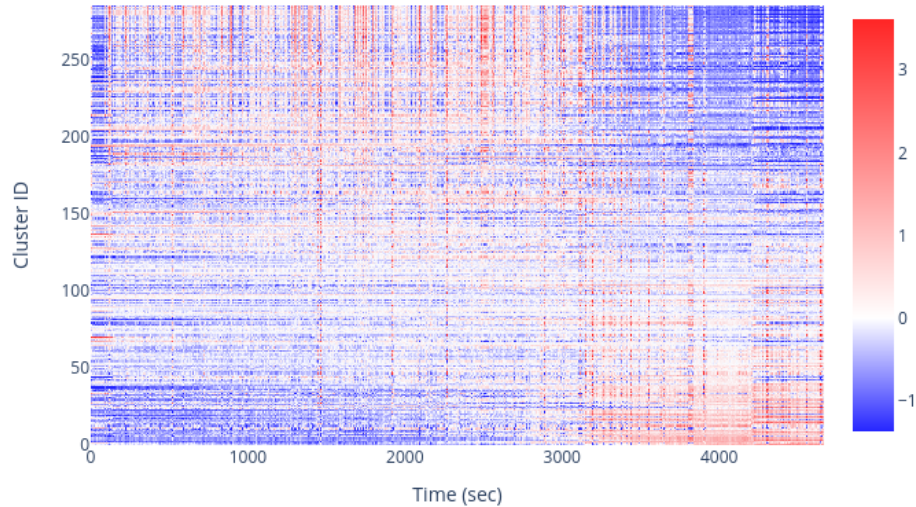


Figure 20: Low-rank approximation of the image in Figure 4 using a truncated SVD or rank 14. Same format as that in Figure 7. Click on the image to access its interactive version.

analytical error: 902.0506743406764, empirical error: 902.0506743406763

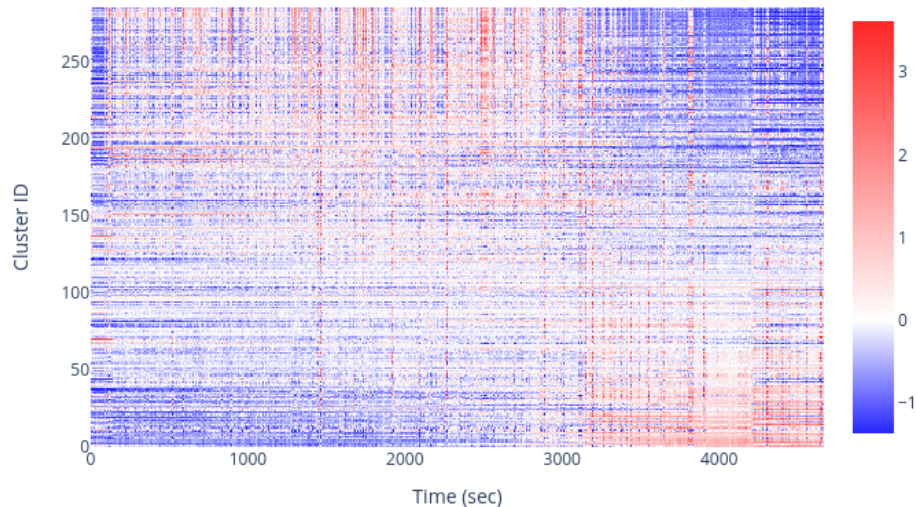


Figure 21: Low-rank approximation of the image in Figure 4 using a truncated SVD or rank 15. Same format as that in Figure 7. Click on the image to access its interactive version.

analytical error: 897.3928573397975, empirical error: 897.3928573397973

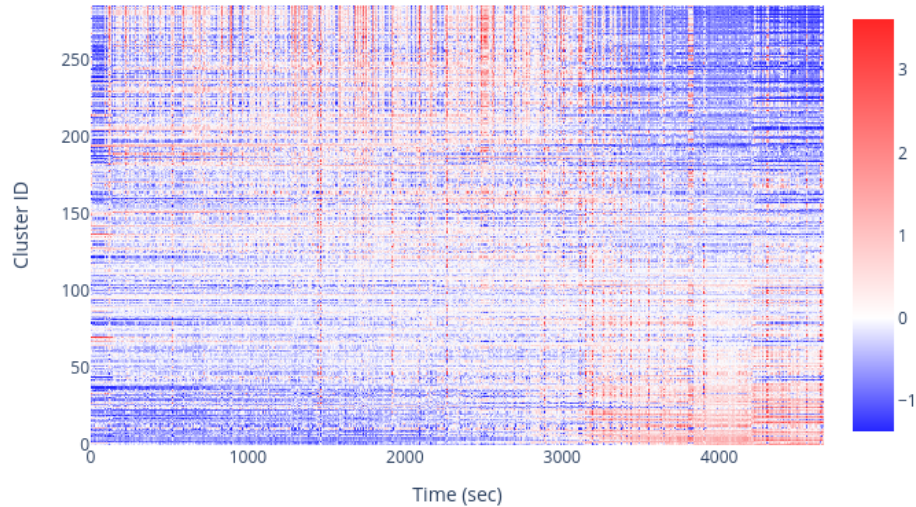


Figure 22: Low-rank approximation of the image in Figure 4 using a truncated SVD or rank 16. Same format as that in Figure 7. Click on the image to access its interactive version.

analytical error: 892.7837887293219, empirical error: 892.7837887293218

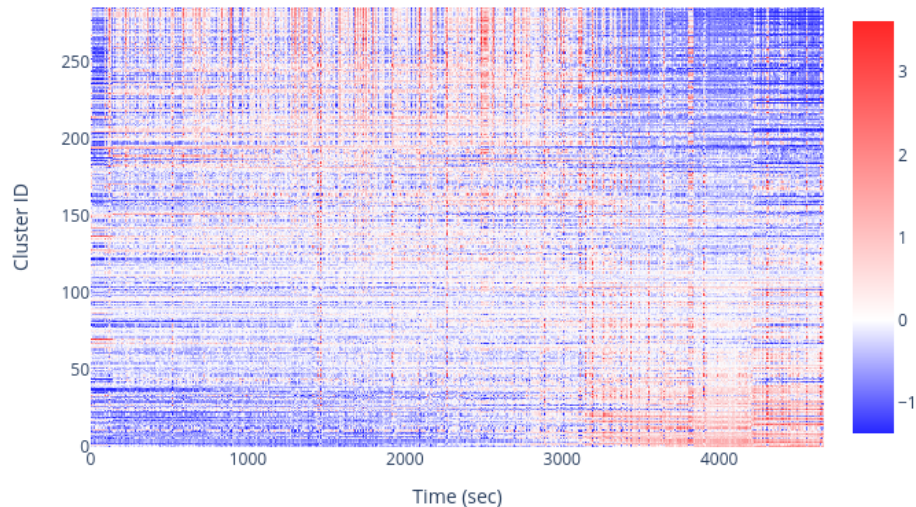


Figure 23: Low-rank approximation of the image in Figure 4 using a truncated SVD or rank 17. Same format as that in Figure 7. Click on the image to access its interactive version.

analytical error: 888.2157053436599, empirical error: 888.2157053436598

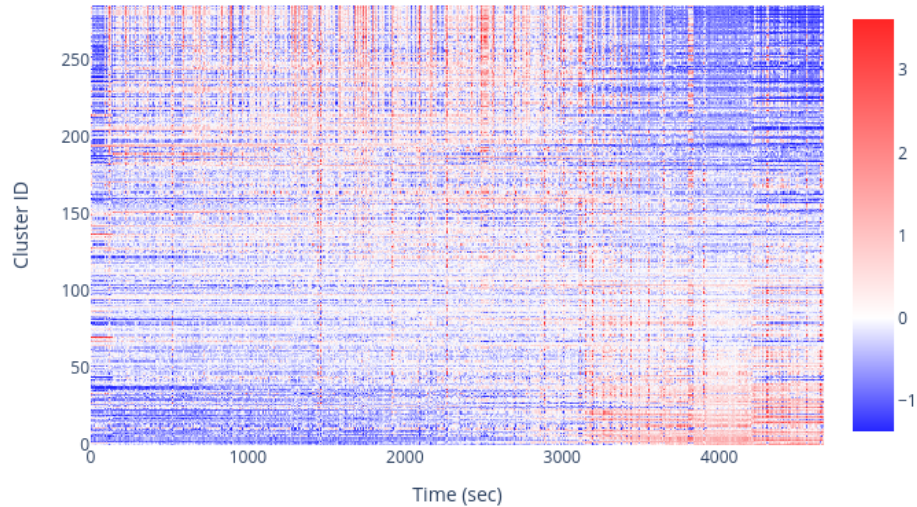


Figure 24: Low-rank approximation of the image in Figure 4 using a truncated SVD or rank 18. Same format as that in Figure 7. Click on the image to access its interactive version.

analytical error: 883.8764673289731, empirical error: 883.8764673289729

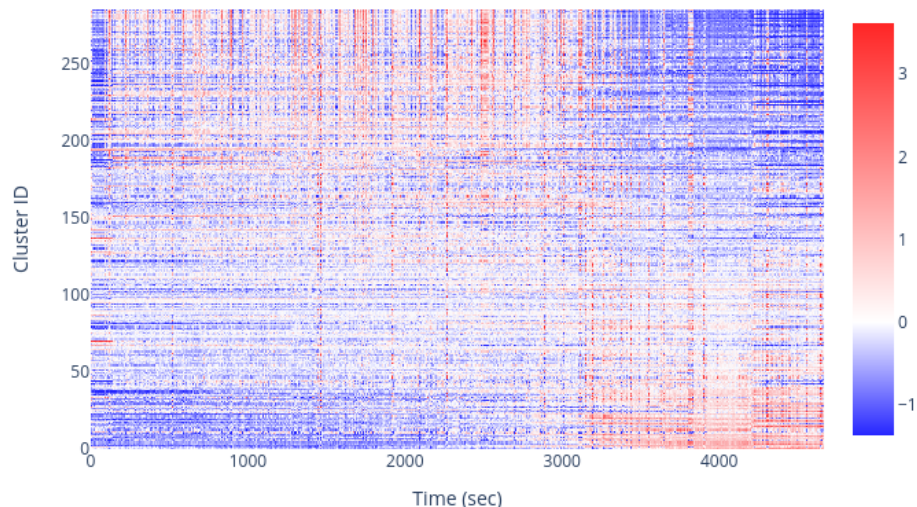


Figure 25: Low-rank approximation of the image in Figure 4 using a truncated SVD or rank 19. Same format as that in Figure 7. Click on the image to access its interactive version.

analytical error: 879.5469472834334, empirical error: 879.5469472834333

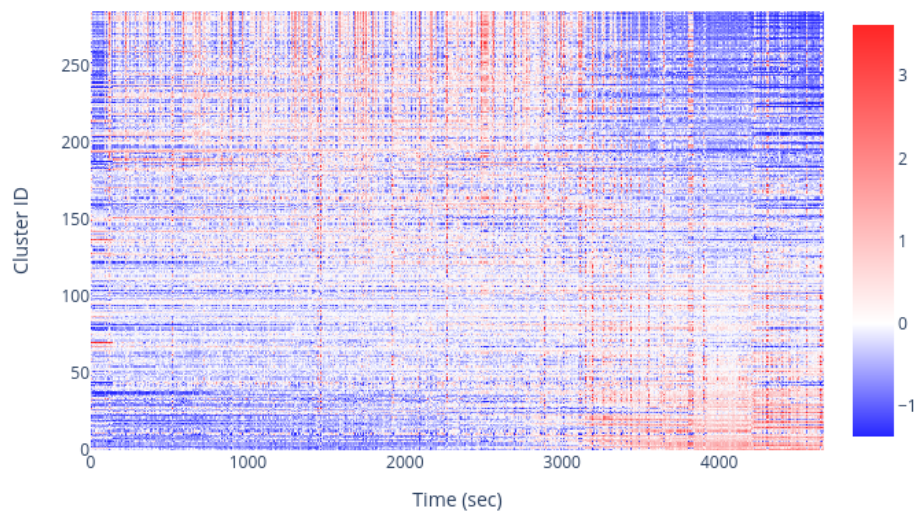


Figure 26: Low-rank approximation of the image in Figure 4 using a truncated SVD or rank 20. Same format as that in Figure 7. Click on the image to access its interactive version.